PARTICLE BEAM DYNAMICS IN A MAGNETICALLY INSULATED COAXIAL DIODE

V.G. Korenev, I.I. Magda, V.G. Sinitsin
National Science Center "Kharkov Institute of Physics and Technology", Kharkov, Ukraine
E-mail: magda@kipt.kharkov.ua

The dynamics of charged particle beams emitted from a cathode into a smooth coaxial diode with magnetic insulation is studied with the aid of 3-D PIC simulation. The processes controlling space charge formation and its evolution in the diode are modeled for geometries typical of high-voltage millimeter wave magnetrons that are characterized by very high values of emission currents, hence high space charge densities.

PACS: 52.75.Pv; 52.80.Pi

INTRODUCTION

The dynamics of charged particles in cross-field devices has for decades been a subject of intense investigations [1-5]. The theme has gained special significance with the advent of high-voltage devices, relativistic magnet-rons in particular, which are characterized by extreme emission currents, high densities of the space charge and great velocities of the electron flows – both in the interaction space and out of it. The importance of this problem stems from the practical necessity to mitigate the tendency toward reduced efficiency of relativistic devices, as compared with the conventional magnet-rons [2], which is particularly noticeable in the high-frequency part of the microwave band [7]. To compre-hend the effects due to space charge in a structure of 'full cylindrical geometry', we have focused on a smo-oth-core model of the magnetron with static ***E*** and ***B*** fields combined so as to ensure absence of the anode current (magnetically insulated operation mode). Earlier papers on the subject (e.g., [3]) have provided a result of considerable significance, namely that in the pre-ocillation (zero anode current) regime of the magnetron the electron flow may be very different from the classic Brillouin flow. This finding followed from a 2-D PIC simulation of a decimeter wave magnetron, involving a modest number (about $3{\cdot}10^4$) of the macroparticles, all of which retained their planar trajectories wihin respective cross-section planes. In contrast to that, at millimeter wavelengths the space charge-induced effects become essentially three dimensional, because of the smaller size of the device and greater emission cur-rents. The electric field vector and the flow velocity acquire components along the structure's axis, in fact very soon after start of the emission process (Fig. 1). The orbits of individual particles are commensurate in size (Larmor radius) with the cathode-anode gap.

1. PARTICLE FLOW DYNAMICS

1.1. MODEL DESCRIPTION

The dynamics of the non-neutral (negatively charged) plasma existing in the coaxial diode has been studied with the help of the 3-D PIC code *CST Particle Studio*, taking full account of the self-fields produced by the macroparticles. The diode was represented by two coaxi-al circular electrodes extending 50 mm along the *z*-axis of the cylindrical polar frame (ρ, φ, z) associated with the diode. The perfectly conducting inner electrode was 15 mm in diameter, while the size of the outer electrode varied between dia=18 mm and dia=28 mm. In some of the simulations the outer electrode (anode) possessed a finite electric conductivity, σ=$5.8{\cdot}10^7$ S/m. Particles with a constant *e/m* ratio (that of the electron) were emitted into the cathode-anode gap from a narrow annular strip (Δz=6 mm) on the surface of the cathode, in the form of mono-energetic packets, W=4.5 eV. The number of point-sized centers of emission on the strip was 1800, and the total number of (macro)particles in the diode's operating space was in excess of three million (up to $5.9{\cdot}10^6$, see Fig. 1). The simulation code permitted modeling the emission current only as gradu-ally changing, from zero to a certain rated magnitude, over a finite rise time (the values were 1 kA or 100 A and 4 ns, respectively). The radial-oriented external electric field was produced by applying a dc voltage across the cathode-anode gap (-340 kV at the cathode and 0 at the anode). The focusing magnetic field of axial orientation was varied around B_0=0.4 T, so as to pro-vide, together with the dc electric field, for either full or partial magnetic insulation.

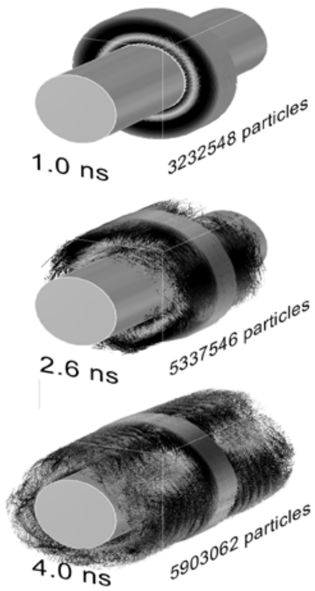

Fig. 1. Process of diode filling by charged (macro) particles: nominal emission current I_e=1 kA

1.2. RESULTS AND DISCUSSION

As can be seen from Fig. 1, the particles leaving the cathode take some time to fill the space right above the annular emitting strip, though shorter than the rise time necessary for the emission current to reach an established nominal value. The particle motion is governed both by the external applied fields $\boldsymbol{E_0}$ and $\boldsymbol{B_0}$, and the fields produced by the space charge. As long as the net magnetic field strength B remains equal to or higher than Hull's cutoff magnitude, the particles cannot reach the anode, and the diode remains magnetically insulated (see the lower panel in Fig. 2: The dc magnetic field B_0=0.51 T is capable of maintaining the insulation regime both during the current formation period and through that of steady-state emission). A non-zero anode current through an initially insulated diode may appear owing to the space charge-produced electrostatic field. The situ-ation is shown in the upper panel of Fig. 2 where the ap-plied dc magnetic field of 0.46 T had been sufficient for diverting the particles from the anode until at $t \approx 1.5$ ns the diode became conductive as a result of further build-up in the space charge. Next, the start of two opposite particle flows along the z-axis can be seen at $t \approx 2.6$ ns both in Figs.1, and 2. Till that moment the motion of individual particles was two-dimensional, with each of them moving along a planar trajectory within the diode's cross-section plane (ρ, φ) which it was emitted to. The sum of the anode current and the axial currents, including such to auxiliary structure elements, shall be (and is) equal to the emitted current – however, not the nominal but rather the space charge-controlled value. The latter is formed under dual-stream conditions, with particles moving at each radial distance from the cathode both toward the anode and back. Note the 'real' emission current to settle at a lower level when the flow to the anode is absent.

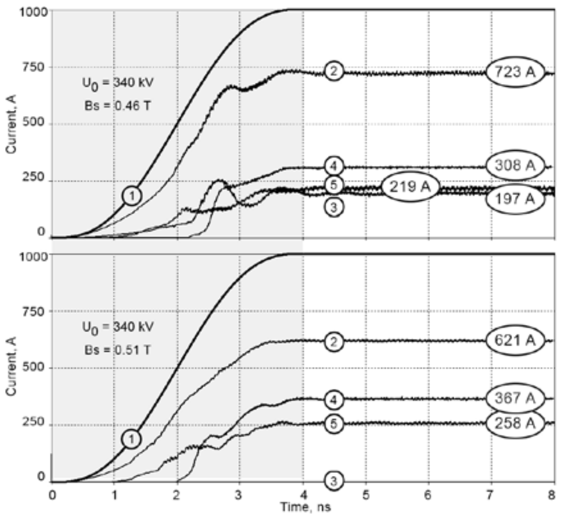

Fig. 2. Balance of currents through the diode (electrode diameters 15, and 28 mm), with a 1 kA nominal emission current, for two magnitudes of the focusing magnetic field: 1 – nominal emission current; 2 – space charge-limited emission current; 3 – current flow to the anode; 4 – total current of axially directed flows; 5 – current to structure supports, etc

The motion of the non-neutral plasma can be described, in the cold fluid approximation, by the equation

$$\frac{d\boldsymbol{p}}{dt} = e\boldsymbol{E} + \frac{\boldsymbol{p} \times \boldsymbol{B}}{mc}, \qquad (1)$$

where $\boldsymbol{p}$ is momentum of the fluid element and m its mass. By projecting (1) to the (ρ-φ) plane, it is easy to derive the 'radial force equilibrium' equation [6],

$$-\gamma \frac{mV_\varphi^2}{\rho} = eE_\rho + \frac{e(V_\varphi B_z - V_z B_\varphi)}{c}, \qquad (2)$$

with $\gamma = [1-(V_\varphi^2 + V_z^2)/c^2]^{1/2}$. Here γ is the relativistic factor, $E\rho$ stands for the radial component of the electric field vector, and $V_\varphi = \omega(\rho)\rho$ is the azimuthal velocity, with $\omega(\rho)$ the respective angular velocity of the rotating 'hub' of particles. The magnetic component B_z includes both the applied field and the self-induced, axially oriented contribution. The azimuthal component B_φ is fully self-induced, owing to the space charge, and is often neglected in analyses of plasma equilibria and instabilities [3, 4]. Apparently, this may be plausible at an early stage of the process when no axial flow has formed yet, $V_z \approx 0$ and B_φ is small, *i.e.* in the case of Fig. 2 at times earlier than 2.2 or 2.3 ns. Space charge density simulations for these early periods are shown in Fig. 3 where the left-hand column presents results for a nominal emission current of 100 A and the right-hand one for 1 kA, all in the coaxial structure with a cathode of ρ_c=7.5 mm and anode, ρ_a =14 mm (15 mm/28 mm diode), placed in a 0.46 T magnetic field. The charge density distributions refer to the central cross-section plane of the diode, z=0. Estimating representative magnitudes of the plasma frequency, $\omega_p = (4\pi Qe/m)^{1/2}$, and cyclotron frequency, $\omega_H = (e/m)B/c$ (where Q is charge density), from the data of Fig. 3 we find $\omega_H \approx 8\cdot10^{10}$ s^{-1} and ω_p ranging from $0.7\cdot10^{10}$ to $1.5\cdot10^{10}$ s^{-1} in the left column, and $2.4\cdot10^{10}$ to $3.9\cdot10^{10}$ s^{-1} in the right one. The 'self-field parameter' $s_e = 2\omega_p^2/\omega_H^2$ [6] is less than one throughout, which suggests a relatively weak repulsion effect of the space charge against the focusing action of the magnetic field, owing to the low charge density at early stages of the process. Meanwhile, even at this early stage the laminar Brillouin flow condition,

$$\omega_p^2(\rho) = \omega_H^2[1 - \frac{1}{2}(\frac{\rho_b{}^4 - \rho_c^4}{\rho_b{}^4})] \qquad (3)$$

($\rho_b \le \rho_a$ is the beam radius), known for the transverse (2-D) motion of the particles [6], is not met. The squared plasma frequency ω_p^2 which is proportional to charge density Q remains less than the magnitude in the right-hand side of (3) because of the axial outflow of particles. Within each cross-section, the radial profiles of space charge density are, on the average, close to a parabola, which they should be in the relativistic case [4], and demonstrate several points of change in the sign of $\partial Q/\partial\rho$ between the cathode and the anode. On the one hand, these changes may be regarded as indicators of a developing diocotron (slipping stream) instability which gives rise to azimuthal waves $\sim \exp(in\varphi - i\omega t)$ around the plasma column.

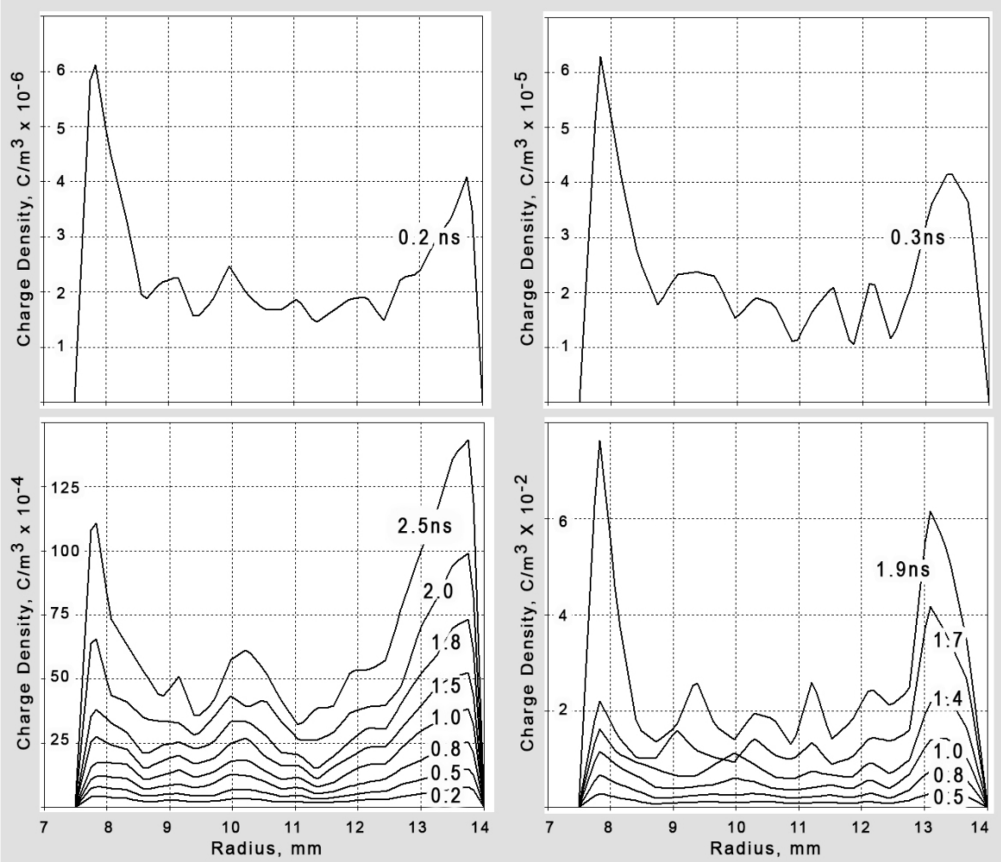

Fig. 3. Radial space-charge density distributions in the 15/28 mm diode, at several successive instants during the early stage of hub formation. Left column: nominal emission current I_e =100 A; right column: I_e =1 kA. The changes in the sign of $\partial Q / \partial \rho$ within the C-A gap, where Q is charge density, indicate conditions for the development of the diocotron instability

On the other hand, a suspicion remains that the radial non-uniformity of the early-stage charge density might be an effect arising from the discrete model of the emission. Assuming that the instability does evolve, we expect the waves with n = 1, 2, 3, *etc.* to be overlaid on the general rotational motion of the plasma hub.

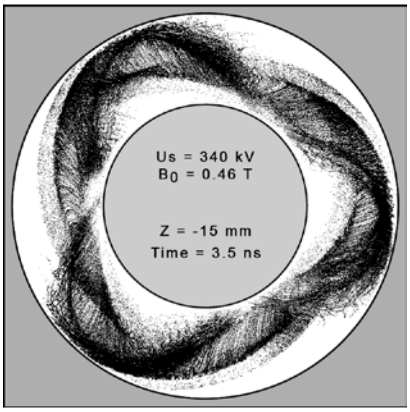

Fig. 4. Cross-sectional view of charge density distribution in the 15/28 mm diode, featuring a n=3 azimuthal wave. With B_0 =0.46 T, the degree of magnetic insulation is close to 'critical' and $\rho_b \approx \rho_a$ =14 mm

Figs. 4 and 5 show the faceted particle patterns that have developed at later times (t>3 ns) from the unstable density profiles like in Fig. 3. The number n of the preferred azimuthal mode, hence the quantity of facets, is determined by the effective thickness of the plasma beam along the radial, *i.e.* by the ratio ρ_c/ρ_b, where the beam radius ρ_b may be less than or equal to the radius of the anode, depending on the degree of magnetic insulation. The 'critical' insulation in Fig. 4 where the plasma barely touches to the anode gives rise to an almost equilibrium state of the particle beam with three broad 'rays' of charge density, *i.e.* the preferred azimuthal mode is n =3. The case of Fig. 5 is characterized by a smaller width of the cathode-anode gap (the anode radius is 12 mm rather than 14 mm), plus a noticeably higher magnetic field, B_0 = 0.707 T.

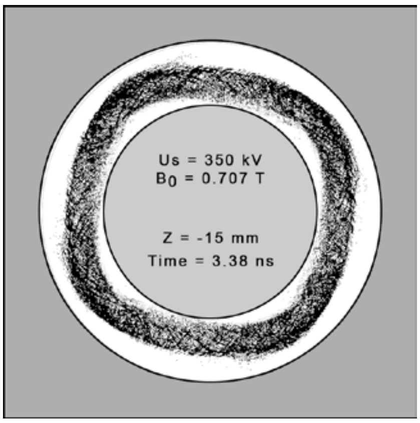

Fig. 5. Cross-sectional view of charge density distribution in the 15/24 mm diode, featuring a n=4 azimuthal wave. The full magnetic insulation with B_0=0.707 T results in a $\rho_b < \rho_a$ =12 mm

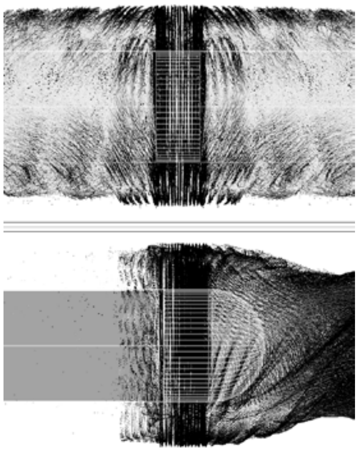

Fig. 6. Axially accelerated particles and formation of annular beams away from the emitter. The upper panel represents a diode with a full-sized coaxial cathode, and the lower one shows an asymmetric pattern in a structure with a 'shortened' electrode

As a result, in the fully insulated beam the cross-sectional density distribution takes the form of a rounded tetragon, n=4. By further reducing the gap width, we could obtain charge density patterns (and the corresponding distributions of the electric self-fields) characteristic of higher-order azimuthal modes, for example n=12 for ρ_c =11 mm. These peripheral waves are not confined to the axial limits of the emitting strip on the cathode but propagate along the z-axis, giving rise to a (hollow) annular particle beam. The azimuthal patterns are retained in the near-surface layers of the propagating beam, taking the form of helical traces. Examples of such annular beams are given in Fig. 6 which shows simulation results for a coaxial diode with a 'full sized' cathode (upper panel) and for a diode with a cathode cut off at one end. In the upper panel, it can be seen that the beam particles gradually emerge from the area near the emitter, where their motion was predominantly two-dimensional, and acquire z-component of velocity under the action of the space-charge field. This axially oriented acceleration reveals itself particularly brightly in the asymmetric pattern of particle positions presented in the lower part of Fig. 6. The radial size of the beam reduces non-uniformly along z away from the emitter because of the now existing axial current and its associated azimuthal magnetic field.

The ensemble of particles rotating in the diode at angular velocities ω= (2…3)·10^{10} 1/s should be capable of exciting some of the proper oscillations pertinent to the diode as a wave supporting structure (a resonant cavity or section of a transmission line). Indeed, oscillatory regimes for currents and the cathode-anode voltage happened to appear at times about 2 ns or 2.5 ns, *i.e.* well before the diode space has been completely filled with the particles. Analysis of dispersive proper-ties and excitation characteristics would be more appropriate if it were a realistic magnetron model with a slow wave structure in one of the electrodes, however a few remarks concerning the present model are in order. The oscillation frequencies excited are close, though not equal, to estimated eigenfrequencies of an empty transmission line of the same cross-section as the diode. Both amplitudes and "exact" frequencies of the oscillations are dependent on the amount of magnetic insulation or, rather, on the effective size of the particle hub which determines the transverse (radial) eigenvalues. Examples of the oscillations appearing under different conditions in the 15/28 mm diode are given in Fig. 7 in a spectral representation. The smaller effective sizes of the plasma column (*i.e.*, higher magnetic fields) correspond to higher oscillation frequencies.

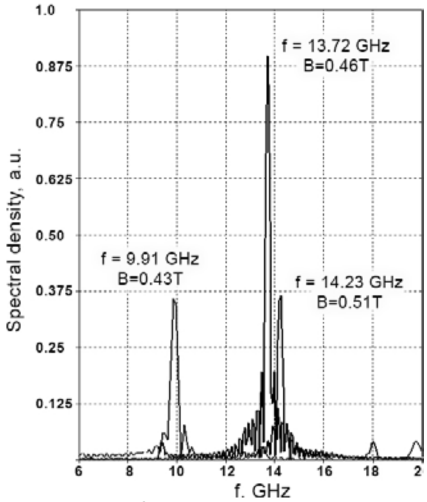

Fig. 7. Spectra of C-A voltage oscillations in the 15/28 mm diode with various magnitudes of the applied magnetic field

CONCLUSIONS

The motion of charged particles in the high voltage, smooth-core coaxial diode operated in the regime of either full or partial magnetic insulation is essentially three-dimensional, and largely different in the 2-D cross-sectional area from the laminar Brillouin flow dynamics.

The space-charge density distribution along the radial coordinate is not monotonic, being modified by relativistic effects and axial outflow of particles. The equilibrium distributions are established with account of axial motion of the particles.

The particles moving in the axial direction are accelerated by the self-field of the space charge, and ultimately give rise to an annular beam with a helical density structure on the outer surface.

REFERENCES

1. O. Buneman. *Crossed-field microwave devices* / ed. F. Okress, v. 1. New York: Academic Press, 1961, p. 209.
2. F.J. Agee. Evolution of Pulse Shortening Research in Narrow Band, High Power Microwave Devices // *IEEE Trans. Plasma Sci.* 1998, v. 26, p. 235.
3. H.-W. Chan, C. Chen, R.C. Davidson. Numerical study of relativistic magnetrons // *J. Appl. Phys*. 1993, v. 73, № 11, p. 7053-7060.
4. I. Kotelnikov, M. Romé, R. Pozzoli. On the relativistic cold fluid radial equilibrium of a nonneutral plasma // *Physics Letters A.* 2008, v. 372, iss. 9, p. 1445-1450.
5. Y.Y. Lau, J.W. Luginsland, K.L. Cartwright, D.H. Simon, W.Tang, B.W. Hoff, R.M. Gilgenbach.

A re-examination of the Buneman-Hartree condition in a cylindrical smooth-bore relativistic magnetron // *Phys. Plasmas*. 2010, v. 17, 033102; doi: 0.1063/1.3328804.
6. R.C. Davidson. *Physics of non-neutral plasmas*. New York, Addison-Wesley. 1992, p. 290-310.
7. S.A. Berdin, K.V. Chizhov, N.P. Gadetski, V.G. Korenev, A.N. Lebedenko, M.I. Marchenko, I.I. Magda, O.G. Melezhik, V.G. Sinitsin, V.A. Soshenko. Special traits of the millimeter wave relativistic magnetron // *Problems of Atomic Science and Technology. Series "Nuclear Physics Investigations"*. 2014, № 3, p. 54-59.

Article received 17.06.2015

ДИНАМИКА ПУЧКОВ ЗАРЯЖЕННЫХ ЧАСТИЦ В КОАКСИАЛЬНОМ ДИОДЕ С МАГНИТНОЙ ИЗОЛЯЦИЕЙ

В.Г. Коренев, И.И. Магда, В.Г. Синицын

Методом трехмерного численного моделирования исследуется динамика пучка заряженных частиц, эмиттируемых с катода в коаксиальный диод с магнитной изоляцией. Процессы, определяющие формирование и эволюцию пространственного заряда, моделируются для такой геометрии диодной структуры, которая характерна для высоковольтных магнетронов миллиметрового диапазона. Эти приборы отличаются очень высокими эмиссионными токами и, соответственно, высокими значениями плотности нескомпенсированной плазмы. Рассмотрены процессы развития плазменных неустойчивостей, которыми определяется распределение плотности заряда и электромагнитного поля в системе.

ДИНАМІКА ПУЧКІВ ЗАРЯДЖЕНИХ ЧАСТИНОК У КОАКСІАЛЬНОМУ ДІОДІ З МАГНІТНОЮ ІЗОЛЯЦІЄЮ

В.Г. Коренєв, І.І. Магда, В.Г. Сініцин

Шляхом тривимірного чисельного моделювання досліджено динаміку пучка заряджених частинок, які емітовані з катоду в коаксіальний діод з магнітною ізоляцією. Процеси, які визначають формування та еволюцію просторового заряду, моделюються для таких геометричних параметрів діодної структури, що є характерними для високовольтних магнетронів міліметрового діапазону. Такі пристрої відрізняються дуже високим емісійним струмом, отже, високими значеннями щільності некомпенсованої плазми. Розглянуто розвиток плазмових нестійкостей, що ними визначається розподіл зарядів та електромагнітного поля в системі.